JOURNAL OF NEUROTRAUMA
Volume 23, Number 9, 2006

Pp. 1304–1319

Neuronal Response to High Rate Shear Deformation Depends on Heterogeneity of the Local Strain Field

D. KACY CULLEN and MICHELLE C. LaPLACA

ABSTRACT

Many cellular models of traumatic brain injury (TBI) deform cells in a planar (2-D) configuration, a contrast from the three-dimensional (3-D) architecture of the brain, resulting in strain fields that may fail to represent the complex deformation patterns seen *in vivo*. Cells cultured in 3-D may more accurately represent *in vivo* cellular behavior than planar models due to differences in cytostructure, cell-cell/cell-matrix interactions and access to trophic factors; however, the effects of culture configuration on the response to high rate deformation have not been evaluated. We examined cell viability following a defined mechanical insult to primary cortical neurons distributed throughout a bioactive matrix (3-D) or in a monolayer sandwiched between layers of a bioactive matrix (2-D). After high rate loading (20 or 30 sec^{-1}; 0.50 strain), there was a significant decrease in neuron viability for both configurations versus unloaded control cultures; however, neurons in 3-D presented greater cell death based on matched bulk loading parameters. Computer simulations of bulk loading predicted local cellular strains, revealing that neurons in 3-D were subjected to a heterogeneous strain field simultaneously consisting of tensile, compressive and shear strains; conversely, neurons in 2-D experienced a less complex deformation regime varying mainly based on shear strains. These results show differential susceptibility to mechanical loading between neurons cultured in 2-D and 3-D that may be due to differences in cellular strain manifestation. Models of TBI that accurately represent the related cellular biomechanics and pathophysiology are important for the elucidation of cellular tolerances and the development of mechanistically driven intervention strategies.

Key words: cell mechanics; neuron; shear strain, strain rate; traumatic brain injury

INTRODUCTION

TRAUMATIC BRAIN INJURY (TBI) is caused by a mechanical insult to the head and may result in temporary or permanent brain dysfunction. After a mechanical insult to brain tissue, cells may undergo immediate death if structural thresholds are surpassed; however, secondary cellular alterations may be initiated in surviving cells that can progress for weeks to months after the insult (Gennarelli, 1997; McIntosh et al., 1998). As a result, functional impairment may be prolonged due to altered signaling cascades and the limited regenerative ability of the brain. Rapid acceleration/deceleration of the head (inertial loading) has been shown to produce tissue strain throughout the brain, and has been linked to such clinical manifestations as diffuse brain injuries (Margulies et

Wallace H. Coulter Department of Biomedical Engineering, Parker H. Petit Institute for Bioengineering and Bioscience, Laboratory for Neuroengineering, Georgia Institute of Technology, Emory University, Atlanta, Georgia.

al., 1990; Margulies and Thibault, 1992; Gennarelli, 1993). Although previously reported *in vitro* models of TBI are able to recreate various aspects of primary and secondary damage in a controlled setting, such models have ranging physiological and biomechanical relevance to clinical head injury (Morrison et al., 1998b). Models include deformable membranes that are stretched biaxially (Ellis et al., 1995; Cargill and Thibault, 1996; Geddes and Cargill, 2001) or uniaxially (Pfister et al., 2003; Lusardi et al., 2004) to transfer deformation to attached cells, some with the capability of deforming neurites aligned longitudinally to the strain field (Smith et al., 1999). In such models, difficulty may exist in correlating membrane strain with individual cell strain due to variable cell adhesion to the deformable substrate. Furthermore, a commonality between these models of neural trauma is that they deform cells primarily via tension; however, the physical properties of brain tissue make shear the dominant mode of deformation upon mechanical loading since brain tissue has a high bulk modulus and a low shear modulus (Holbourn, 1943; Sahay et al., 1992). Devices utilizing shear deformation have been developed; for instance, hydrodynamic models utilizing fluid shear to deform cells (LaPlaca and Thibault, 1997b; Nakayama et al., 2001). The aforementioned models have primarily been utilized to deform cells in a planar (2-D) orientation, which may limit the ability to simulate complex strain combinations. Also, the one-sided distribution of cellular adhesions found in 2-D cultures may affect pathological mechanotransduction mechanisms. Models of neural trauma utilizing cells arranged in a three-dimensional (3-D) configuration may better recapitulate the biomechanics of traumatic loading to the brain, which results in the generation of complex, heterogeneous strain fields at the tissue and cellular levels. *In vitro* models have been developed to evaluate the injury response in brain tissue slices—thus preserving the 3-D configuration (Morrison et al., 1998a; Sieg et al., 1999; Adamchik et al., 2000). However, in these models the ability to control cellular and extracellular matrix (ECM) constituents are limited, thus making the mechanistic elucidation of the roles of specific factors in the injury response difficult.

Correlating the extent of cell death and functional impairment with the mechanical parameters inducing brain injury is crucial to elucidate cellular tolerances and secondary responses. Models of neural trauma that injure cells distributed in 3-D throughout an ECM may more faithfully recapitulate such secondary responses than planar cultures lacking a surrounding ECM. Interpretation of cellular responses in 2-D models may be confounded by fundamental differences in terms of the cellular microenvironment (e.g., access to trophic factors), atypical cellular morphology (Balgude et al., 2001; Grinnell, 2003), and altered cell-cell/cell-matrix interactions (Cukierman et al., 2001, 2002; Schmeichel and Bissell, 2003; Yamada et al., 2003). In traditional 2-D cultures, the sink-like property of the bathing medium may serve to dilute secreted or released molecules at the time of injury; conversely, 2-D cultures have demonstrated an increase in sensitivity to chemical treatments independent of changes in surface area (Miller et al., 1985), possibly making 2-D models less suitable for studies evaluating pharmacological intervention after neural trauma. Models of neural trauma utilizing a 3-D cellular configuration may therefore be a more accurate representation of the *in vivo* situation based on enhanced physiological and biomechanical relevance while maintaining the experimental control of previous *in vitro* systems. Accordingly, such neuronal culture configurations, with the potential for cell-cell and cell-matrix interactions in all spatial dimensions, may provide a useful setting in which to investigate the effects of 3-D strain transfer to individual cells.

The goal of the current study was to evaluate the response between neuronal cultures plated in two configurations to a defined, high rate mechanical insult. The two configurations evaluated were (1) neurons homogeneously distributed throughout a bioactive matrix material (500–600 μm thick)—termed "3-D"; or (2) neurons plated in a monolayer horizontal plane sandwiched between layers of a bioactive matrix material (total thickness of 500–600 μm)—termed "2-D." Prior to experiments subjecting these cultures to mechanical loading, comparisons were made between neurons cultured in 2-D and 3-D to establish baseline parameters having potential ramifications on the injury response, such as culture viability, cell morphology, neuronal marker expression, neurite outgrowth and astrocyte composition. Following baseline characterization, neuronal cultures were subjected to high rate deformation and alterations in cell viability were assessed as a function of loading parameters. Furthermore, simulations of representative cellular strain fields were generated to gain insight into the cellular biomechanics of high strain rate induced cell death for neurons cultured in 2-D versus 3-D. This model presents the unique capability of analyzing the influence of a 3-D, heterogeneous strain field on individual neurons as a function of the predicted local cellular strain regime.

METHODS

Cortical Neuron Harvest and Dissociation

Procedures involving animals were approved by the Institutional Animal Care and Use Committee (IACUC)

of the Georgia Institute of Technology. Neurons were obtained from timed-pregnant (embryonic day 17) Sasco Sprague-Dawley rats (Charles River, Wilmington, MA). Anesthetized dames were rapidly decapitated and the uterus was removed by Caesarian section and placed in Hanks Balanced Salt Solution (HBSS; Invitrogen, Carlsbad, CA). Each fetus was removed from the amniotic sac, rapidly decapitated, and the brains removed. The cortices were isolated and placed in pre-warmed trypsin (0.25%) + 1 mM EDTA (Invitrogen) for 10 min at 37°C. The trypsin-EDTA was removed and the tissue was tritutated in HBSS + DNase I (0.15 mg/mL; Sigma, St. Louis, MO) using a flame-narrowed Pastuer pipet. The tissue was then centrifuged at 1000 rpm for 3 min, and the cells were resuspended in a defined medium (Neurobasal medium + 2% B-27 + 500 μM L-glutamine [Invitrogen]).

Two-Dimensional and Three-Dimensional Primary Cortical Neuronal Cultures

Primary cortical neuronal cultures were generated in 2-D (monolayer sandwiched between two layers of matrix) and 3-D (homogeneously dispersed throughout matrix) in cell chambers designed to interface with a custom-built injury device. Prior to plating, chambers were pre-treated with 0.05 mg/mL poly-L-lysine (PLL; Sigma) followed by Matrigel® (0.5 mL/well at 0.6 mg/mL; Becton Dickinson Biosciences, Bedford, MA) in Neurobasal medium (each treatment was >4 h). This pre-treatment provides a thin layer of matrix between the glass substrate and the neuronal cultures promoting cellular adhesion. Neurons cultured in 3-D were plated within Matrigel® (final protein concentration of 7.5 mg/mL) at a cell density of 3750–5000 cells/mm^3 (corresponding to 4.5–6.0 $\times$ 10^5 cells distributed throughout a 500–600-μm-thick matrix; Fig. 1). Cultures were placed at 37°C to permit matrix gelation and 3-D cell entrapment. For 2-D neuronal cultures, cells were plated at a planar cell density of 1250–2500 cells/mm^2 (corresponding to 3.0–6.0 $\times$ 10^5 cells) in 0.5 mL of medium. After allowing for neuronal adhesion, Matrigel® (7.5 mg/mL) was placed above the 2-D cultures to match the amount of matrix used in the 3-D system; thus, the 2-D cultures were a monolayer with matrix below, as well as 500–600 μm of matrix above. After matrix gelation in 2-D and 3-D cultures, 0.5 mL of warm medium was added per culture. Cultures were maintained at 37°C and 5% CO_2-95% humidified air, and fed at 24 h post-plating and every 2–3 days thereafter. All experiments were performed at 7–8 days *in vitro* (DIV). The cell density range used for 3-D culture was based on optimized neuronal viability (data not shown), whereas the cell density range chosen for 2-D culture was based on approximating the number of cells seeded in the 3-D cultures while maintaining baseline viability near 90%.

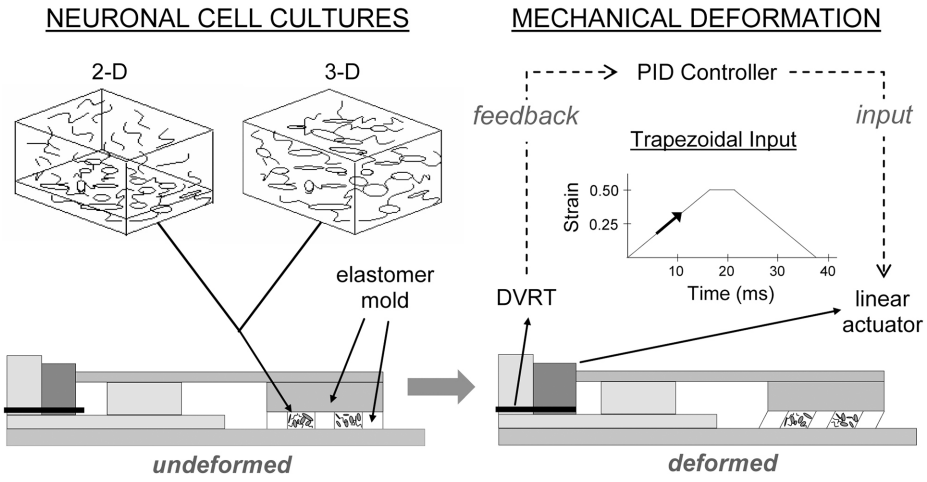

FIG. 1. Schematic representation of the neuronal culture (left) and mechanical deformation (right) models (not to scale). Neuronal cultures in planar (2-D) and three-dimensional (3-D) configurations were plated above a layer of acellular matrix and were laterally constrained by an elastomer mold. 3-D neuronal cultures were homogeneously dispersed throughout a bioactive matrix, whereas 2-D neuronal cultures were plated and, after allowing for cell adhesion, were covered with additional bioactive matrix. Mechanical deformation was imparted to cell-containing matrices through the action of the 3-D Cell Shearing Device (CSD), a custom-built electromechanical device. A closed-loop control system (PID controller with positional feedback from a DVRT) governs a linear actuator, causing horizontal displacement of the cell chamber top-plate inducing shear deformation in the elastomer mold and cell-imbedded matrices.

Cell Viability Using Fluorescent Staining

Neuron viability was assessed using fluorescent probes for distinguishing live and dead cells. Cell cultures were incubated with 4 μM ethidium homodimer-1 (EthD-1) and 2 μM calcein AM (both from Molecular Probes, Eugene, OR) at 37°C for 30 min and then rinsed with 0.1 M Dulbecco's phosphate-buffered saline (DPBS; Invitrogen). The percentage of viable cells was calculated by counting the number of live cells (fluorescing green by AM-cleavage) and the number of cells with compromised membranes (nuclei fluorescing red by EthD-1).

Phenotypic Identification Using Immunocytochemistry

Neuronal cultures were immunostained using primary antibodies recognizing the following intracellular proteins: (1) tau-5 (MS247P, 1:200; NeoMarkers, Fremont, CA), a microtubule-associated protein expressed predominantly in maturing neurons (Binder et al., 1985; Migheli et al., 1988; Nunez, 1988; Goedert et al., 1991) or (2) glial fibrillary acidic protein (GFAP; AB5804, 1:400; MAB360, 1:400; Chemicon, Temecula, CA), an intermediate filament found in astrocytes (Debus et al., 1983). Briefly, cells were fixed in 3.7% formaldehyde (Fisher, Fairlawn, NJ) for 30 min, rinsed in PBS, and permeabilized using 0.3% Triton X100 (Kodak, Rochester, NY) containing 4% goat serum (Invitrogen) for 20 min. Primary antibodies were added (in PBS + 4% serum) at 18–24°C for 4 h. After rinsing, the appropriate secondary fluorophore-conjugated antibodies (FITC or TRITC-conjugated IgG, Jackson Immuno Research, West Grove, PA or Alexa 488 or 546-conjugated IgG, Molecular Probes; each 1:500) were added (in PBS + 4% serum) at 18–24°C for 2 h. Hoechst 33258 (1:1000; Molecular Probes) was used as a counterstain. The percentage of neurons in culture was assessed by determining the numbers of tau$^+$ cells versus the total number of cells (n = 4 in 3-D, and n = 8 in 2-D). Similarly, the percentage of astrocytes was assessed by counting the number of GFAP$^+$ cells (n = 6 in 2-D, and n = 5 in 3-D).

Mechanical Loading Using the Three-Dimensional Cell Shearing Device

Neuronal cultures in 2-D and 3-D were mechanically loaded using the 3-D Cell Shearing Device (CSD), a custom-built electromechanical device capable of quantifiably imparting high rate shear deformation to 3-D cell-containing matrices (LaPlaca et al., 2005). At the time of injury, cultures were removed from the incubator and mounted within the 3-D CSD. The mechanical action of the device was driven by a linear-actuator (BEI Kimco, San Marcos, CA) governed by a proportional-integral-derivative (PID) (Feedback Inc., Hillsborough, NC) controller with closed-loop motion control feedback from a differential variable reluctance transducer (DVRT, Microstrain; Burlington, VT) (Fig. 1). A trapezoidal input was provided by custom code written in LabVIEW® (National Instruments, Austin, TX) software. Cultures plated in 2-D were deformed (strain 0.50, strain rate 20 sec^{-1}, n = 16; strain 0.50, strain rate 30 sec^{-1}, n = 11) or placed into the device with the top plate (static control, n = 14). Cultures plated in 3-D were deformed (strain 0.50, strain rate 20 sec^{-1}, n = 12; strain 0.50, strain rate 30 sec^{-1}, n = 17) or placed into the device with the top plate (static control, n = 17). After mechanical deformation, warm medium was added and the cultures were returned to the incubator. Viability was also assessed in naïve control cultures in 2-D (n = 11) and 3-D (n = 11).

Simulations of Local Cellular Strain Using Matlab®

A kinematic analysis of the strain field generated by the 3-D CSD was previously performed to relate the bulk deformation of the matrix to the applied local cellular strain dependent on soma/neurite orientation within the matrix (LaPlaca et al., 2005). This work is extended here to theoretically compare the local cellular strain fields experienced by neurons in 2-D versus 3-D culture conditions. The orientation of a soma/neurite within the matrix was defined based on a fixed Cartesian reference frame as the initial angles projected into the x_3,x_2 plane and in the x_1,x_2 plane (denoted as $\phi \in [-90°,90°]$ and $\alpha \in [-90°,90°]$, respectively) (Fig. 2). In

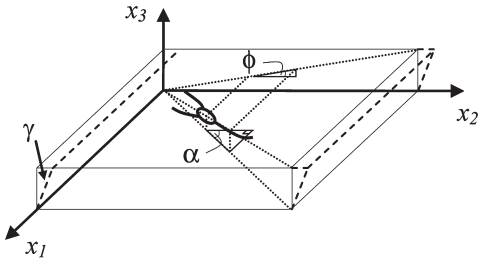

FIG. 2. Description of cell orientation used in theoretical strain analysis. The orientation of a neuron was described based on the departure angle from horizontal (defined as ϕ, a projection into the x_3,x_2 plane) and the angle from vertical (defined as α, a projection into the x_1,x_2 plane). The shear deformation of the cell-containing matrices (proportional to the angle γ) occurs in the x_3,x_2 plane. The Green's strain tensor describing the bulk deformation of the matrix was translated to a local cellular strain using a series of rotational transformations. This methodology permits the determination of the components of the Green's strain tensor specific for a soma/neurite at any orientation with respect to the strain field induced by the 3-D CSD.

order to support this analysis, evaluation of the morphology and cytostructure of neurons in 2-D and 3-D cultures was performed using high resolution confocal microscopy. Specifically, confocal z-stacks were acquired across the full thickness of the cultures. The orientation angles describing the departure trajectory of neurites from the soma were measured from neurons in 2-D and 3-D ($n = 12$ neurons each from four cultures, with a range of 1–9 neurites per neuron). This was accomplished using Zeiss Image Browser by transforming the z-stacks into 3-D reconstructions and aligning the viewing plane to correspond to the x_3,x_2 plane or the x_1,x_2 plane and manually measuring ϕ or α, respectfully, using the angle measurement feature. The local normal and shear strains for neurites at discrete orientation angles within the strain field generated by the 3-D CSD were then calculated using a custom simulation written in Matlab®.

Statistical Analysis

After viability and immunocytochemistry assays, cells were viewed using fluorescent microscopy techniques on an epifluorescent microscope (Eclipse TE300, Nikon, Melville, NY) or a confocal laser scanning microscope (LSM 510, Zeiss, Oberkochen, Germany). For

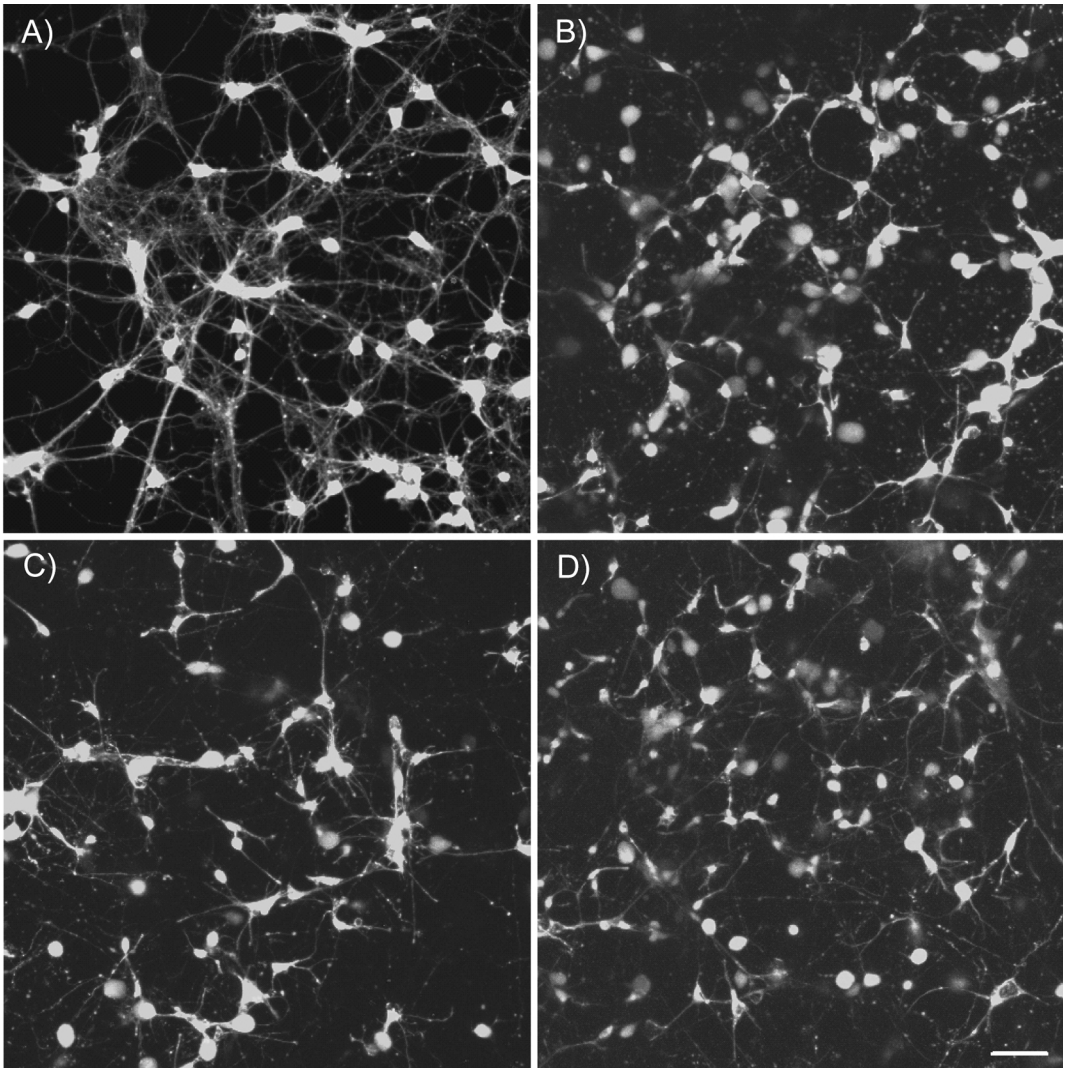

FIG. 3. Baseline viability in planar (2-D) and three-dimensional (3-D) neuronal cultures. Representative fluorescent confocal reconstructions of neuronal cultures plated in 2-D (**A**) or in 3-D configurations dispersed throughout matrix, with representative reconstructions taken from the bottom (**B**), middle (**C**), or top (**D**) of the cultures (100-μm-thick sections each). Cultures were stained to denote live cells. There was not a significant difference between neuronal viability based on culture configuration. Scale bar = 50 μm.

epifluorescent microscopy, images were digitally captured (DKC5T5/DMC, Sony, Tokyo, Japan) and analyzed using Image-Pro Plus (Media Cybernetics, Silver Spring, MD). Confocal images were processed and analyzed using LSM Image Browser and AxioVision (both Zeiss). Confocal images were acquired across the full thickness of the cultures, permitting calculation of the overall culture thickness occupied by cells and the culture viability and cell density as functions of matrix depth. Three to five randomly selected regions per culture were counted for statistical analysis. Data are presented as mean ± standard deviation (σ). For analysis of baseline culture parameters and post-loading viability, general linear model ANOVA was performed and, when significant differences existed between groups, Tukey's pairwise comparisons test was performed ($p < 0.05$ was required for significance for either test). For the theoretical strain analysis, general linear model ANOVA ($p < 0.05$ required for significance) was performed followed by the variance ratio test ($\alpha < 0.01$ required for significance).

Table 1. Cell Culture Viability as a Function of Depth in the Matrix

		Viability (%)	
	Depth	*By depth*	*Overall mean*
2-D	Bottom	92.8 ± 4.0	
	Top	90.0 ± 5.9	
3-D	Middle	90.2 ± 5.0	87.1 ± 7.0
	Bottom	81.2 ± 15.9	

The baseline viability was measured for neurons cultured in planar (2-D) and three-dimensional (3-D) configurations. For neuronal cultures in 3-D, the viability was calculated as a function of depth into the matrix. For these calculations, total thickness z-stacks were binned into 100-μm-thick sections taken from the bottom (closest to glass coverslip), middle, and top (closest to media) of the cultures. There were not statistically significant differences in the viability in 3-D cultures based on depth, nor were there differences in viability in 2-D compared to 3-D cultures. Data are presented as mean ± standard deviation.

RESULTS

Culture Characterization

Neuronal cultures in 2-D and 3-D were evaluated based on viability, morphology, neurite outgrowth, and neuronal/astrocytic composition since baseline culture parameters may influence the neuronal response to high rate deformation. Cells plated in 3-D extended numerous processes at all orientations while cells plated in 2-D remained nearly planar, as expected. In 3-D neuronal cultures, the total culture thickness occupied by cells was measured to be 550.9 ± 28.6 μm. Throughout this thickness, there was not a statistically significant difference in cell viability based on depth (Fig. 3). The mean cell density was determined to be 3608 ± 1280 cells/mm^3, and also did not statistically vary based on depth. Although these data do demonstrate consistent neuronal survival and distribution throughout the thickness of the cultures, the variability in neuronal survival did increase deeper into the constructs, possible indicating limitations in mass transport. However, the overall culture viability for 3-D neuronal cultures did not differ statistically from neuronal cultures plated in 2-D (Table 1). Additionally, both 2-D and 3-D configurations yielded similar percentages of cells staining positive for the maturing isoform of the neuronal cytoskeletal marker tau-5 (~90% each) as well as the astrocyte marker GFAP (~3% each; Fig. 4).

Confocal microscopy revealed morphological and cytostructural differences between neurons distributed throughout a matrix compared to neurons in planar culture. Neurons in 3-D presented a bulbous morphology with neurites departing the soma in all spatial dimensions, whereas neurons in 2-D culture presented a restricted cytostructure with neurites departing the soma mainly in the horizontal plane. Specifically, in a 3-D configuration, neurites were arranged at all possible orientation angles, thus the measured departure trajectories of neurites were found over the full range ($\phi \in [-90°,90°]$ and $\alpha \in [-90°,90°]$). For cultures in a 2-D configuration, the neurite departure angles were not restricted in the horizontal plane ($\alpha \in [-90°,90°]$); however, neurite departure trajectories were found to be restricted in the vertical plane ($\phi \in [-10°,10°]$; Fig. 5). However, there was not a statistically significant difference in the mean number of neurites departing the soma per neuron for neurons plated in 2-D compared to 3-D configurations (4.6 ± 1.5 and 4.1 ± 1.8 neurites/neuron, respectively). Altogether, these results demonstrate differences in neuronal cytoarchitecture in 3-D versus 2-D cultures; however, both configurations produce viable cultures with similar neuronal and astrocytic compositions.

Response to High Rate Deformation

Post-injury cell viability as a function of culture configuration was assessed using a standard live/dead assay in conjunction with confocal microscopy. Cell viability was found to significantly depend on culture configuration (2-D versus 3-D, $p < 0.05$), injury level ($p < 0.001$), and interactions between the two variables ($p < 0.05$), indicating a synergistic dependence between culture con-

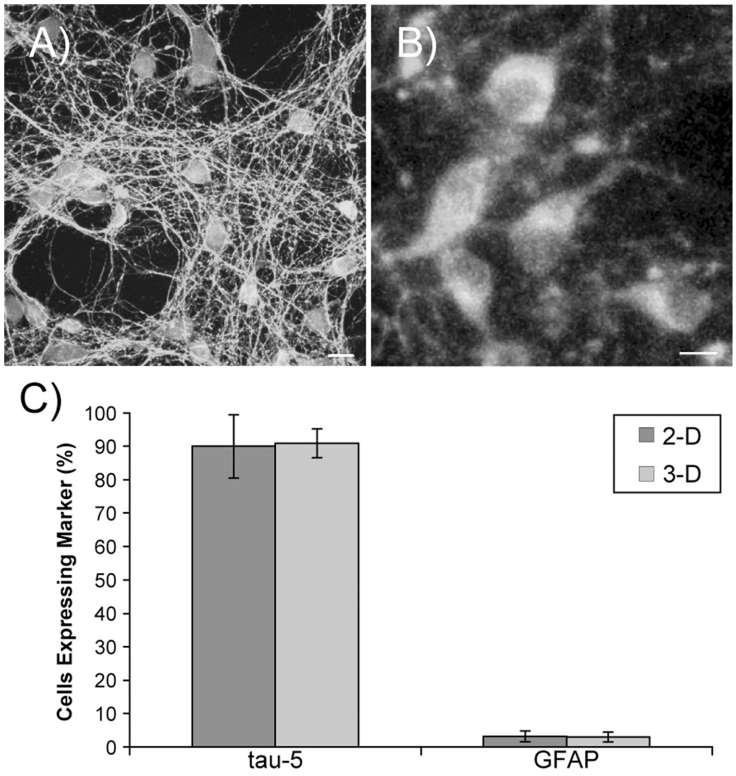

FIG. 4. Neuronal cultures in planar (2-D) and three-dimensional (3-D) configurations were immunolabeled to identify neurons and astrocytes. Representative fluorescent confocal reconstructions of neuronal cultures in 2-D (**A**) or 3-D (**B**) configurations immunolabeled for tau-5 were to denote neurons with Hoechst counterstain. Scale bar = 10 μm. The astrocyte presence was similarly determined by immunolabeling for GFAP (images not shown). (**C**) Graphical representation of the neuron/astrocyte composition based on culture configuration. There was not a significant difference between the percentage of neurons or astrocytes in 2-D and 3-D configurations. Error bars represent standard deviation.

figuration and injury level (Fig. 6). There was not a statistical difference between the static and naive controls in either 2-D or 3-D cultures. For the 2-D cultures, there was a significant decrease in cell viability versus the static control cultures for the 20 sec^{-1}, 0.50 strain injury and 30 sec^{-1}, 0.50 strain injury ($p < 0.05$). Similarly, there was a significant difference in the percentage of viable cells under both loading conditions for the injured 3-D cultures versus the static control 3-D cultures ($p < 0.001$; Fig. 7). There was not a strain rate dependence on viability for the strain rates evaluated in either the 2-D or the 3-D cultures. However, there was a statistically significant decrease in cell viability based on matched loading conditions between the 2-D compared to 3-D cultures, signifying that culture configuration affects the response to high rate deformation.

Simulations of Local Cellular Strain

A kinematic analysis of the strain field generated by the 3-D CSD was performed to theoretically compare the local cellular strains experienced by neurons in a 2-D versus 3-D configuration based on cellular orientation with respect to the bulk deformation of the matrix. Neurite orientation measurements taken from neurons in both configurations were used to calculate the theoretical local cellular strain based on methodology previously described (LaPlaca et al., 2005). Briefly, the bulk deformation of the cell-containing matrix was described by the Green's strain tensor for the case of simple shear deformation where γ is the shear angle (Fig. 2). This bulk strain tensor was transformed to a local strain tensor aligned longitudinally with the orientation of a neurite departing the soma (described by ϕ and α) based on a series of rotational transformations. Thus, the local strain tensor as a function of initial neurite orientation within the matrix is described by:

$$E'_{11} = 0$$

$$E'_{22} = \frac{1}{2}\tan(\gamma)(\sin(2\phi)\cos(\alpha) + \sin^2(\phi)\tan(\gamma))$$

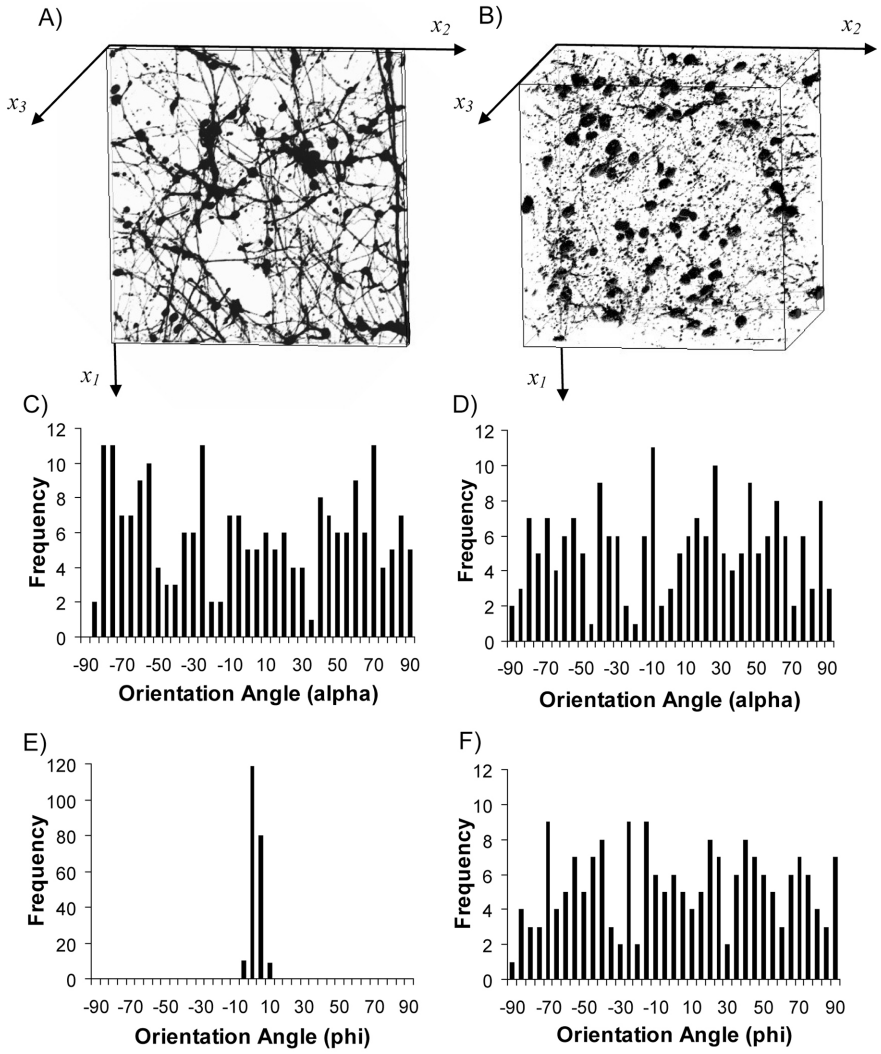

FIG. 5. Histogram of neurite departure trajectories from neurons in planar (2-D) and three-dimensional (3-D) culture. 3-D confocal reconstructions of neuronal cultures plated in 2-D (**A**) and 3-D (**B**) configurations. Scale bar = 50 μm. The angles of neurite departure from the soma in the horizontal plane (α) did not vary between neurons cultured in 2-D (**C**) compared to 3-D (**D**) configurations; i.e., neurites were measured over the full range of $\alpha \in [-90°,90°]$. However, neurite departure angles in the vertical plane (ϕ) were statistically different in 2-D (**E**) versus 3-D (**F**) configurations over all orientation angles ($p < 0.05$) as departure angles were found to be restricted for neurons cultured in 2-D configuration ($\phi \in [-10°,10°]$) whereas neurite departure angles were not restricted for neurons plated in 3-D configuration, ($\phi \in [-90°,90°]$). This signifies that neurons in the encapsulated monolayer configuration had a more restricted cytostructure and that the majority of neurites departed the soma at angles of orientation close to the horizontal plane. This analysis lends insight into neuronal cytoarchitecture when plated in the 2-D versus the 3-D configuration, and was later utilized in the theoretical strain analysis.

$$E'_{33} = \frac{1}{2}\tan(\gamma)(-\sin(2\phi)\cos(\alpha) + \cos^2(\phi)\tan(\gamma))$$
$$E'_{12} = E'_{21} = -\frac{1}{2}\tan(\gamma)\sin(\phi)\sin(\alpha)$$
$$E'_{13} = E'_{31} = -\frac{1}{2}\tan(\gamma)\cos(\phi)\sin(\alpha)$$
$$E'_{23} = E'_{32} = \frac{1}{2}\tan(\gamma)\left(\cos(2\phi)\cos(\alpha) + \frac{1}{2}\sin(2\phi)\tan(\gamma)\right)$$

The local normal strains are the longitudinally aligned axial strain, E'_{22}, and the orthogonally-aligned vertical strain, E'_{33}; the local shear strains are E'_{12} (lateral-shear strain), E'_{13} (vertical-shear strain), and E'_{23} (axial-shear strain). Based on initial orientation, neurites may experience a range of axial and vertical strains resulting in both extension and compression (Fig. 8). These normal strains were found to more variable for neurites in a 3-D con-

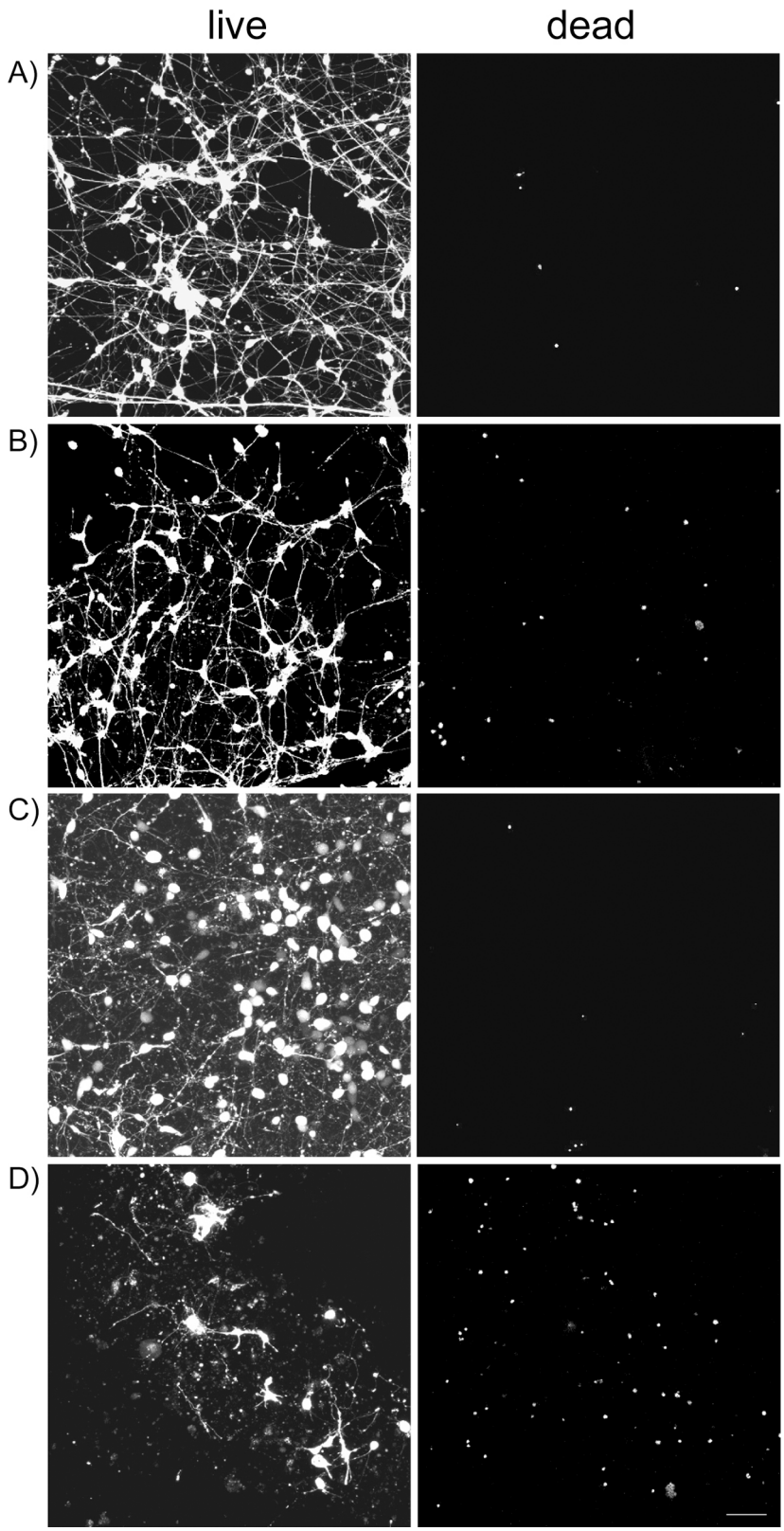

FIG. 6. Post-injury viability in neuronal cultures in planar (2-D) and three-dimensional (3-D) configurations. Cultures were subjected to control conditions or high strain rate and magnitude shear deformation using the 3-D CSD with cell viability assessed 24 h post-insult. Representative fluorescent confocal reconstructions of neuronal cultures in 2-D after static control (**A**) or 0.50 strain, 30 sec^{-1} strain rate (**B**) and neuronal cultures in 3-D after static control (**C**) or 0.50 strain, 30 sec^{-1} strain rate (**D**). Scale bar = 50 μm. There was an increase in cell death following high rate loading in both 2-D and 3-D neuronal cultures compared to static controls.

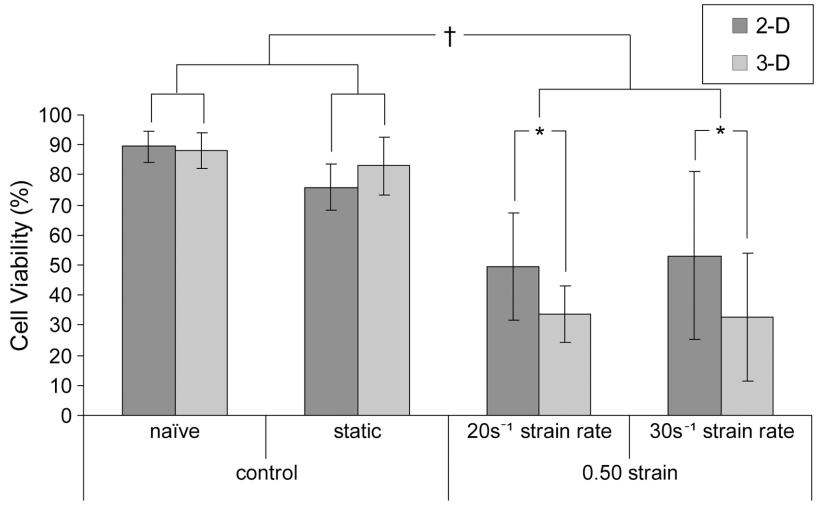

FIG. 7. Post-injury viability in neurons cultured in planar (2-D) and three-dimensional (3-D) configurations. Neuronal viability was assessed 24 h following high rate deformation or control conditions. There was not a significant difference in viability in naïve controls compared to static controls for either 2-D or 3-D; however, there was a significant decrease in both 2-D and 3-D viability after high rate deformation. *Indicates a significant decrease in viability in 2-D versus 3-D under matched loading conditions ($p < 0.05$). †Indicates a significant decrease in viability versus uninjured controls ($p < 0.05$). Error bars represent standard deviation.

figuration compared to 2-D. Specifically, the longitudinally-aligned axial strain and the orthogonal vertical strain were relatively consistent for neurites in the 2-D configuration ($\sigma = 0.03$) compared to neurites in 3-D ($\sigma = 0.31$), and this increase in variability was statistically greater for neurites in 3-D ($\alpha < 0.01$). Moreover, axial strains were close to zero for the majority of the neurites in 2-D, and were thus statistically higher for neurites in 3-D ($p < 0.001$). Thus, the only significant normal strains experienced by neurons in 2-D were vertical strains, acting orthogonal to a given neurite departure trajectory. Shear strains followed similar trends as those described for normal strains. The magnitude and variability of axial-shear strains and vertical-shear strains were similar for neurites in 2-D and 3-D. However, lateral-shear strains were greater for neurites in 3-D ($p < 0.001$) and had a greater variability ($\alpha < 0.01$). Thus, strain fields experienced by neurons plated in 2-D were in general more homogeneous and included significant axial-shear strains with low axial strains (Fig. 9A). Conversely, for neurons in 3-D, arbitrary combinational strain fields were experienced, including those dominated by axial strains (i.e., extension and compression) or those dominated by axial-shear strains, potentially varying between neurites from the same neuron (Fig. 9B). Furthermore, considering dynamic loading conditions as the matrix is driven from an undeformed state ($\gamma = 0°$) to a state of maximum deformation ($\gamma = 45°$), the strain continuum of a neurite may result in continuous extension, continuous compression, or initial compression followed by extension, but such strain fields were only possible for neurites in a 3-D configuration. It may be the simultaneous application of complex strain fields, consisting of significant normal and shear elements, which results in maximal neuronal damage, and such combinational strains fields were found primarily in a 3-D configuration.

DISCUSSION

A novel model of TBI has been developed to subject cell cultures plated in 2-D or 3-D to bulk shear deformation to allow for direct comparison based on culture configuration. Prior to evaluating the cellular response to mechanical loading, neurons cultured in 2-D and 3-D were characterized to establish a baseline in culture composition and viability as these factors may contribute to the injury response. There were no significant differences in culture viability, number of neurites per neuron, or neuron/astrocyte composition based on culture configuration; however, there were cytostructural differences in neurons cultured in a 3-D versus 2-D configuration. After high magnitude, high rate loading, there was a significant decrease in viability for neurons cultured in both 2-D and 3-D; however, there was a significant decrease in culture viability in 3-D compared to 2-D under matched loading parameters. Simulations to predict the local cellular strains for representative neurons plated in

2-D and 3-D determined that neurons in 3-D experience a heterogeneous strain regime simultaneously consisting of complex combinations of multiple normal and shear strain components; conversely, neurons in 2-D experience a more homogenous strain regime consisting largely of shear strains with a relatively consistent, single component normal strain. This *in vitro* model of TBI has significant deviations from *in vivo* parameters, such as a near-monotypic cell population and the presence of a laminin/collagen-rich matrix, potentially limiting the appropriate scope of applications of this model. However, this model is capable of incorporating a heterogeneous strain regime, representative of the *in vivo* situation, while controlling the culture configuration, matrix constituents, and cellular composition in a simplified setting—thus presenting a degree of experimental control that may be further exploited for the mechanistic elucidation of the contribution of the aforementioned parameters in the injury response.

For these studies, we chose to focus on large magnitude, high rate deformation regimes, and our results did not reveal a dependence on strain rate, perhaps due to the limited range of strain rates chosen (20 and 30 sec^{-1}). In addition, both loading rates may be beyond a neuronal rate-dependent threshold for the large strain magnitude tested (0.50). Previous studies using planar neural cultures demonstrated that the response to mechanical loading was dependent upon strain rate and strain magnitude (Cargill and Thibault, 1996; LaPlaca et al., 1997a; Geddes and Cargill, 2001; Geddes et al., 2003a) as well as interactions between these factors (Geddes and Cargill, 2001; Geddes et al., 2003a). The theoretical analysis of local cellular strain applied to our 3-D model of neural trauma revealed variable magnitude normal and shear strains dependent upon neurite/soma orientation with respect to the bulk deformation; however, loading onset times would theoretically remain constant. This may result in a range of loading rates at the cellular level, further adding cell-level variability when data are pooled from an entire culture based on bulk deformation parameters. However, using our 3-D model of neural trauma for a broader range of strain rates, we have previously demonstrated viability dependence on bulk strain rate in 3-D astrocyte cultures (1 and 20 sec^{-1}) (LaPlaca et al., 2005) and in 3-D neuronal-astrocytic co-cultures (1, 10, and 30 sec^{-1}) (Cullen et al., 2005).

Factors affecting the translation of forces from bulk (macro) deformation to cellular (micro) deformation may differ markedly in 3-D versus 2-D configurations. As demonstrated by this study, the neuronal orientation within the bulk strain field, and hence the local cellular strain, influences the post-injury viability of neuronal cultures. However, other factors influencing the related biomechanics should be noted, such as cell morphology, matrix mechanical properties, and cell-matrix/cell-cell interactions which may play differential roles in the transfer of strain to the cells, and/or differential susceptibility to localized stress formations. This study and others have noted variations in cellular morphology and cytostructure between cells grown in 3-D versus 2-D environments (Balgude et al., 2001; Grinnell, 2003), parameters which may directly influence the development of strains on or within cells (Winston et al., 1989; Barbee et al., 1994), possibly contributing to a differential response to mechanical loading in the present study as the neuronal networks in 2-D were constrained within a region parallel to the direction of the bulk deformation. Viscoelastic properties and porosity may affect the strain manifestation at the cell level for cells contained within a 3-D matrix, and such properties may be tailored to approximate that of brain tissue (Shuck and Advani, 1972; Donnelly and Medige, 1997; Darvish and Crandall, 2001). Differences in the types, quantity, and distribution of cell-cell and cell-matrix

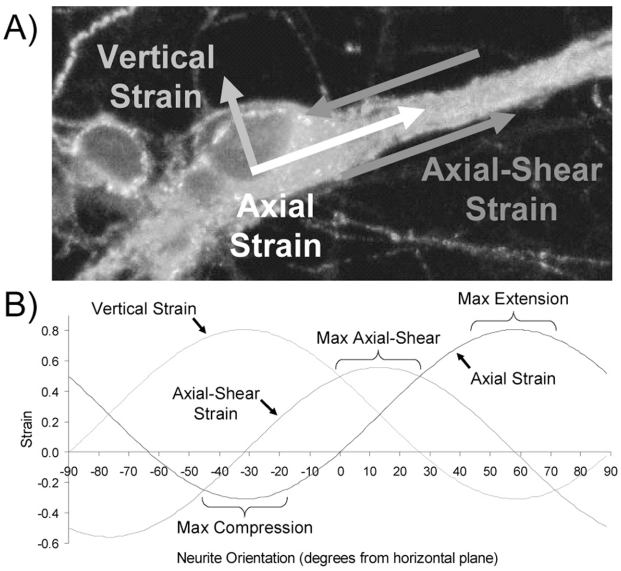

FIG. 8. Demonstration of potential strain fields experienced by cells cultured in planar (2-D) and three-dimensional (3-D) configurations. (**A**) Example of local cellular strain aligned with a neuron. (**B**) Range of theoretical local cellular strains as a function of neurite departure angle from horizontal (ϕ only, α equal to 0° for conceptual simplification). Neurons in 3-D, with departure angles from the horizontal (ϕ) ranging from −90° to 90°, experience a range of potential strain fields consisting of normal (tensile or compressive) and shear strains. However, neurons in 2-D were found to have departure angles from the horizontal contained from −10° to 10°, causing these neurons to experience a more homogeneous strain field.

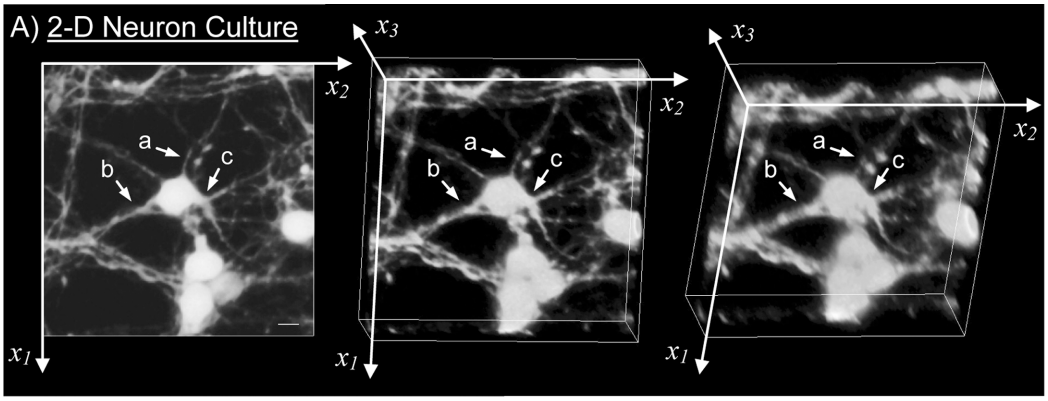

Neurite Orientation Angles

	ϕ	α		ϕ	α		ϕ	α
a	-1.0°	-77.3	b	0.6°	-29.4	c	-2.8°	21.0°

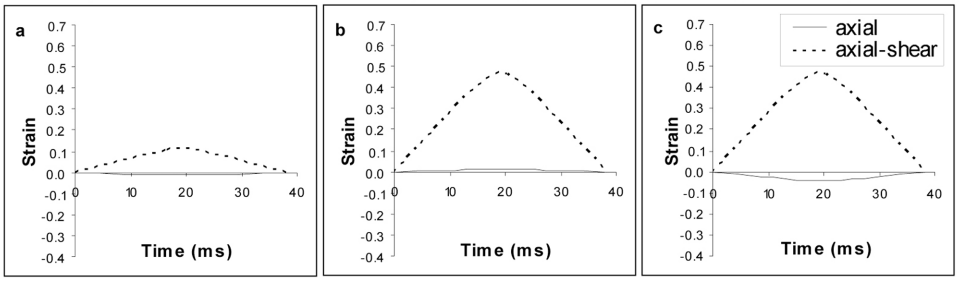

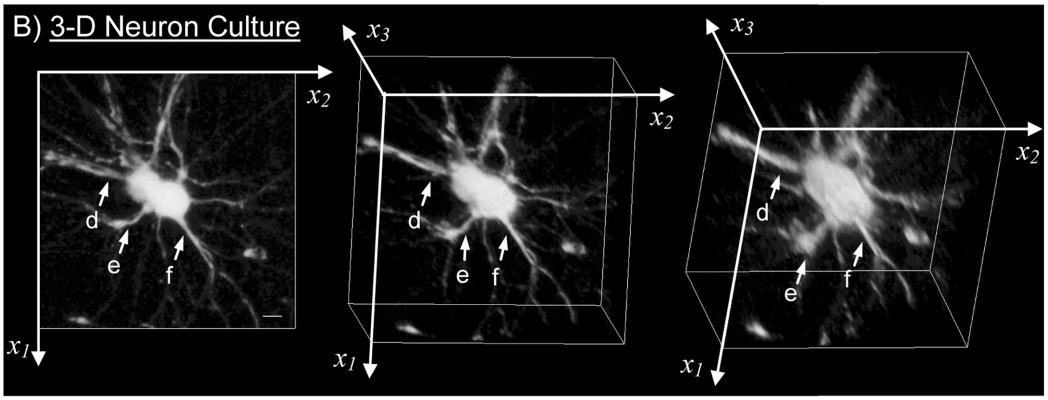

Neurite Orientation Angles

	ϕ	α		ϕ	α		ϕ	α
d	-28.4°	19.5°	e	45.0°	-44.1°	f	9.5°	53.8°

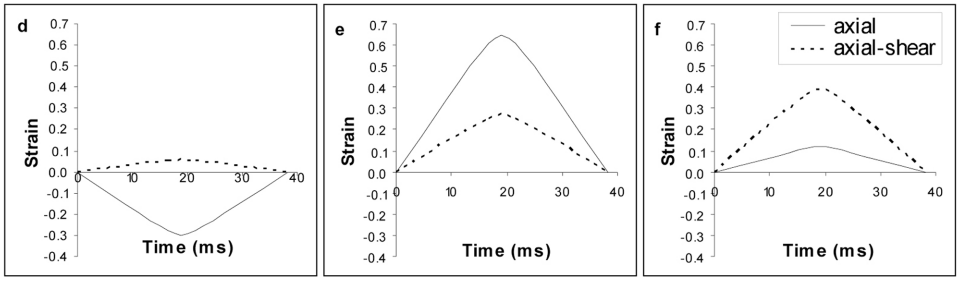

FIG. 9. Local cellular strain simulations for neurons in cultured in planar (2-D) and three-dimensional (3-D) configurations. (**A**) Results of the theoretical strain analysis predicting local cellular strain fields for neurons plated in 2-D. (**a,b,c**) Neurites in 2-D were theoretically subjected to relatively homogeneous strain regimes, generally with high axial-shear strains and low axial strains. (**B**) Neurites projecting from a neuron in 3-D culture were theoretically subjected to variable strains, consisting of strain fields dominated by compressive axial strain (**d**), extensional axial strain (**e**), or axial-shear strain (**f**). Neurons cultured in 3-D experience heterogeneous local cellular strains compared to neurons cultured in 2-D, possibly causing a more detrimental outcome after high rate deformation for neurons in a 3-D configuration. Scale bar = 10 μm.

interactions between cells cultured in 2-D versus 3-D have previously been characterized for various cell types (Cukierman et al., 2001; Schmeichel and Bissell, 2003), supporting the assertion that neurons in a 3-D bioactive matrix will contact matrix factors and experience cell-cell interactions (e.g., receptor-mediated, synaptic) in all spatial directions. Cells in traditional 2-D configurations may experience such interactions in a more limited or one-sided fashion. Receptor-ligand adhesions may serve as areas of stress concentrations, creating regions that are more likely to fail during loading. Such cell-matrix and cell-cell interactions will be a function of the receptor density, receptor clustering, binding strength, and the surface area of the cells. Potential differences in neurite outgrowth for neurons in a 3-D compared to a 2-D configuration may result in a differential contribution of these adhesions on the response to high rate deformation. The effects of cellular orientation, cytoarchitecture, matrix properties, and cell-matrix/cell-cell interactions may work in concert to create the strains and stresses at the cellular level, and these factors may contribute in different proportions in 2-D versus 3-D cell deformation.

The 3-D CSD is able to deliver a bulk shear strain to 3-D cell-containing matrices, the deformation pattern associated with diffuse brain injury, and elicit significant cell death at levels relevant to the *in vivo* injury situation (Gennarelli et al., 1982; Margulies et al., 1990; Margulies and Thibault, 1992). This model may produce a more accurate representation of cell death/dysfunction thresholds than previous 2-D *in vitro* models of TBI due to the 3-D cell orientation and the ability to precisely control the rate and magnitude of the bulk matrix deformation. Bulk tissue shear strains resulting in diffuse axonal injury (DAI) has been approximated to 0.10–0.50 at onset-times corresponding to approximate strain rates of 10–50 sec^{-1} (Margulies and Thibault, 1989; Margulies et al., 1990; Meaney et al., 1995). Neural cellular tolerances to mechanical loading in culture trauma models must be interpreted with caution as model-specific phenomena may result in variable development of stresses and strains, necessitating mechanical inputs far greater than those correlating with *in vivo* injury. For instance, some uniaxial stretch models require strains of >0.50 or rates up to 90 sec^{-1} to elicit axonal pathology (Thibault and Gennarelli, 1989; Smith et al., 1999; Pfister et al., 2003). The rates and magnitudes used in this study were chosen to correspond to those of severe inertial injury, and the degree of cell death in our model at these injury levels indicates a correlation with diffuse brain injury thresholds. Given the results of this study suggesting that local cellular strain may influence the response to bulk mechanical inputs, coupled with the well-documented dependence on strain rate and strain magnitude (Cargill and Thibault, 1996; LaPlaca et al., 1997a; Geddes and Cargill, 2001; Geddes et al., 2003a), it may be proposed that heterogeneity in the neuronal response to bulk mechanical inputs may be due to variations in local stress and strain. Therefore, future derivations of neuronal tolerances to mechanical loading should focus on predictions of local mechanical responses, which may be influenced by cell orientation with respect to the overall strain field, cell and matrix viscoelastic properties, morphology/cytostructure, and cell-cell/cell-matrix adhesions, among other potential factors.

Injuries to the brain are among the most likely traumatic insults to result in death or permanent disability and few, if any, clinically effective treatments exist (Roberts et al., 1998)—facts that substantiate the need for improved laboratory models of TBI. This injury model adds to the repertoire of TBI models as the first capable of generating a controlled, homogeneous deformation to cell-containing matrices where local strain heterogeneity is predictably realized based on the neurite/soma orientation with respect to the overall strain field (LaPlaca et al., 2005). Although stretch models employing brain slices will achieve such heterogeneity in cellular strain (Morrison et al., 1998a), the overall deformation is inherently inhomogeneous due to unconstrained boundary conditions at the top surface, confounding predictions of local cellular strain. *In vitro* models employing planar cultures are valuable in studying the effects of 1-D and 2-D strain fields on neural cultures; however, the ramifications of such simplified strain fields on the acute injury response must be taken into account. For example, non-specific plasma membrane permeability alterations, a generally accepted mechanism of cell injury (Pettus et al., 1994; Pettus and Povlishock, 1996; Singleton and Povlishock, 2004), have been demonstrated *in vitro* when subjecting neurons to biaxial strain regimes (Ellis et al., 1995; LaPlaca et al., 1997a; Geddes et al., 2003a; Geddes-Klein et al., 2006) but only after axotomy in a uniaxial strain field (Smith et al., 1999; Wolf et al., 2001). However, uniaxial stretch models may exploit the unique ability to separate specific modes of altered intracellular ionic homeostasis (e.g., ion channels) from nonspecific modes (e.g., mechanoporation). Also, in 2-D stretch models cell strain may inherently be lower than substrate strain, and variable dependent upon cell adhesion and morphology (Winston et al., 1989; Barbee et al., 1994). Thus, relative levels of cell death or measures of dysfunction between neural cell types may be due to differences in the transfer of substrate strain to cell strain, rather than representing differential loading

thresholds (e.g., cerebral cortical neurons versus hippocampal neurons (Geddes et al., 2003b) and neurons versus astrocytes (Ahmed et al., 2000)).

In summary, subjecting 3-D neural cell cultures to high rate, heterogeneous strain fields may more accurately represent acute responses of cells *in vivo* to a mechanical insult compared to 2-D models of neural trauma, revealing cellular thresholds to loading. The model presented here may be further exploited using 3-D neural cell cultures that take into account more *in vivo* factors (e.g., multicellular composition, matrix constituents, and cell densities more representative of those in the central nervous system) that may serve as a guide to cellular damage/death thresholds while better recapitulating post-injury alterations in cell biochemistry and secondary death mechanisms.

ACKNOWLEDGMENTS

Financial support was partially provided by NSF (CAREER Award BES-0093830), NIH/NIBIB (EB001014), NSF (EEC-9731643) and the Southern Consortium for Injury Biomechanics at the University of Alabama Birmingham-Injury Control Research Center, thru a grant from the National Center for Injury Prevention and Control, Centers for Disease Control and Prevention, Award R49/CE000191 and Cooperative Agreement TNH22-01-H-07551 with the National Highway Traffic Safety Administration.

REFERENCES

ADAMCHIK, Y., FRANTSEVA, M.V., WEISSPAPIR, M., CARLEN, P.L., and PEREZ VELAZQUEZ, J.L. (2000). Methods to induce primary and secondary traumatic damage in organotypic hippocampal slice cultures. Brain Res. Brain Res. Protoc. **5,** 153–158.

AHMED, S.M., RZIGALINSKI, B.A., WILLOUGHBY, K.A., SITTERDING, H.A., and ELLIS, E.F. (2000). Stretch-induced injury alters mitochondrial membrane potential and cellular ATP in cultured astrocytes and neurons. J. Neurochem. **74,** 1951–1960.

BALGUDE, A.P., YU, X., SZYMANSKI, A., and BELLAMKONDA, R.V. (2001). Agarose gel stiffness determines rate of DRG neurite extension in 3D cultures. Biomaterials **22,** 1077–1084.

BARBEE, K.A., MACARAK, E.J., and THIBAULT, L.E. (1994). Strain measurements in cultured vascular smooth muscle cells subjected to mechanical deformation. Ann. Biomed. Eng. **22,** 14–22.

BINDER, L.I., FRANKFURTER, A., and REBHUN, L.I. (1985). The distribution of tau in the mammalian central nervous system. J. Cell Biol. **101,** 1371–1378.

CARGILL, R.S., 2nd, and THIBAULT, L.E. (1996). Acute alterations in $[Ca^{2+}]i$ in NG108-15 cells subjected to high strain rate deformation and chemical hypoxia: an *in vitro* model for neural trauma. J. Neurotrauma **13,** 395–407.

CUKIERMAN, E., PANKOV, R., STEVENS, D.R., and YAMADA, K.M. (2001). Taking cell-matrix adhesions to the third dimension. Science **294,** 1708–1712.

CUKIERMAN, E., PANKOV, R., and YAMADA, K.M. (2002). Cell interactions with three-dimensional matrices. Curr. Opin. Cell Biol. **14,** 633–639.

CULLEN, D.K., SIMON, C.M., and LaPLACA, M.C. (2005). Mechanical induction of degeneration and reactive astrogliosis in three-dimensional neuronal-astrocytic co-cultures. J. Neurotrauma **22,** 1250.

DARVISH, K.K., and CRANDALL, J.R. (2001). Nonlinear viscoelastic effects in oscillatory shear deformation of brain tissue. Med. Eng. Phys. **23,** 633–645.

DEBUS, E., WEBER, K., and OSBORN, M. (1983). Monoclonal antibodies specific for glial fibrillary acidic (GFA) protein and for each of the neurofilament triplet polypeptides. Differentiation **25,** 193–203.

DONNELLY, B.R., and MEDIGE, J. (1997). Shear properties of human brain tissue. J. Biomech. Eng. **119,** 423–432.

ELLIS, E.F., McKINNEY, J.S., WILLOUGHBY, K.A., LIANG, S., and POVLISHOCK, J.T. (1995). A new model for rapid stretch-induced injury of cells in culture: characterization of the model using astrocytes. J. Neurotrauma **12,** 325–339.

GEDDES-KLEIN, D.M., SCHIFFMAN, K.B., and MEANEY, D.F. (2006). Mechanisms and consequences of neuronal stretch injury *in vitro* differ with the model of trauma. J. Neurotrauma **23,** 193–204.

GEDDES, D.M., and CARGILL, R.S., 2nd. (2001). An *in vitro* model of neural trauma: device characterization and calcium response to mechanical stretch. J. Biomech. Eng. **123,** 247–255.

GEDDES, D.M., CARGILL, R.S., 2nd, and LaPLACA, M. C. (2003a). Mechanical stretch to neurons results in a strain rate and magnitude-dependent increase in plasma membrane permeability. J. Neurotrauma **20,** 1039–1049.

GEDDES, D.M., LaPLACA, M.C., and CARGILL, R.S., 2nd. (2003b). Susceptibility of hippocampal neurons to mechanically induced injury. Exp. Neurol. **184,** 420–427.

GENNARELLI, T.A. (1993). Mechanisms of brain injury. J. Emerg. Med. **11,** S5–S11.

GENNARELLI, T.A. (1997). The pathobiology of traumatic brain injury. The Neuroscientist **3,** 73–81.

GENNARELLI, T.A., THIBAULT, L.E., ADAMS, J.H., GRAHAM, D.I., THOMPSON, C.J., and MARCINCIN, R.P. (1982). Diffuse axonal injury and traumatic coma in the primate. Ann. Neurol. **12,** 564–574.

GOEDERT, M., CROWTHER, R.A., and GARNER, C.C. (1991). Molecular characterization of microtubule-associated proteins tau and MAP2. Trends Neurosci. **14,** 193–199.

GRINNELL, F. (2003). Fibroblast biology in three-dimensional collagen matrices. Trends Cell Biol. **13,** 264–269.

HOLBOURN, A.H.S. (1943). Mechanics of head injury. The Lancet **2,** 438–441.

LAPLACA, M.C., CULLEN, D.K., MCLOUGHLIN, J.J., and CARGILL, R.S., 2nd. (2005). High rate shear strain of three-dimensional neural cell cultures: a new *in vitro* traumatic brain injury model. J. Biomech. **38,** 1093–1105.

LAPLACA, M.C., LEE, V.M., and THIBAULT, L.E. (1997a). An *in vitro* model of traumatic neuronal injury: loading rate-dependent changes in acute cytosolic calcium and lactate dehydrogenase release. J. Neurotrauma **14,** 355–368.

LAPLACA, M.C., and THIBAULT, L.E. (1997b). An *in vitro* traumatic injury model to examine the response of neurons to a hydrodynamically-induced deformation. Ann. Biomed Eng. **25,** 665–677.

LUSARDI, T.A., RANGAN, J., SUN, D., SMITH, D.H., and MEANEY, D.F. (2004). A device to study the initiation and propagation of calcium transients in cultured neurons after mechanical stretch. Ann. Biomed. Eng. **32,** 1546–1558.

MARGULIES, S.S., and THIBAULT, L.E. (1989). An analytical model of traumatic diffuse brain injury. J. Biomech. Eng. **111,** 241–249.

MARGULIES, S.S., and THIBAULT, L.E. (1992). A proposed tolerance criterion for diffuse axonal injury in man. J. Biomech. **25,** 917–923.

MARGULIES, S.S., THIBAULT, L.E., and GENNARELLI, T.A. (1990). Physical model simulations of brain injury in the primate. J. Biomech. **23,** 823–836.

MCINTOSH, T.K., SAATMAN, K.E., RAGHUPATHI, R., GRAHAM, D.I., SMITH, D.H., LEE, V.M., and TROJANOWSKI, J.Q. (1998). The Dorothy Russell Memorial Lecture. The molecular and cellular sequelae of experimental traumatic brain injury: pathogenetic mechanisms. Neuropathol. Appl. Neurobiol. **24,** 251–267.

MEANEY, D.F., SMITH, D.H., SHREIBER, D.I., BAIN, A.C., MILLER, R.T., ROSS, D.T., and GENNARELLI, T.A. (1995). Biomechanical analysis of experimental diffuse axonal injury. J. Neurotrauma **12,** 689–694.

MIGHELI, A., BUTLER, M., BROWN, K., and SHELANSKI, M.L. (1988). Light and electron microscope localization of the microtubule-associated tau protein in rat brain. J. Neurosci. **8,** 1846–1851.

MILLER, B.E., MILLER, F.R., and HEPPNER, G.H. (1985). Factors affecting growth and drug sensitivity of mouse mammary tumor lines in collagen gel cultures. Cancer Res. **45,** 4200–4205.

MORRISON, B., 3rd, MEANEY, D.F., and MCINTOSH, T.K. (1998a). Mechanical characterization of an *in vitro* device designed to quantitatively injure living brain tissue. Ann. Biomed. Eng. **26,** 381–390.

MORRISON, B., 3rd, SAATMAN, K.E., MEANEY, D.F., and MCINTOSH, T.K. (1998b). *In vitro* central nervous system models of mechanically induced trauma: a review. J. Neurotrauma **15,** 911–928.

NAKAYAMA, Y., AOKI, Y., and NIITSU, H. (2001). Studies on the mechanisms responsible for the formation of focal swellings on neuronal processes using a novel in vitro model of axonal injury. J. Neurotrauma **18,** 545–554.

NUNEZ, J. (1988). Immature and mature variants of MAP2 and tau proteins and neuronal plasticity. Trends Neurosci. **11,** 477–479.

PETTUS, E.H., CHRISTMAN, C.W., GIEBEL, M.L., and POVLISHOCK, J.T. (1994). Traumatically induced altered membrane permeability: its relationship to traumatically induced reactive axonal change. J. Neurotrauma **11,** 507–522.

PETTUS, E.H., and POVLISHOCK, J.T. (1996). Characterization of a distinct set of intra-axonal ultrastructural changes associated with traumatically induced alteration in axolemmal permeability. Brain Res. **722,** 1–11.

PFISTER, B.J., WEIHS, T.P., BETENBAUGH, M., and BAO, G. (2003). An *in vitro* uniaxial stretch model for axonal injury. Ann. Biomed. Eng. **31,** 589–598.

ROBERTS, I., SCHIERHOUT, G., and ALDERSON, P. (1998). Absence of evidence for the effectiveness of five interventions routinely used in the intensive care management of severe head injury: a systematic review. J. Neurol. Neurosurg. Psychiatry **65,** 729–733.

SAHAY, K.B., MEHROTRA, R., SACHDEVA, U., and BANERJI, A.K. (1992). Elastomechanical characterization of brain tissues. J. Biomech. **25,** 319–326.

SCHMEICHEL, K.L., and BISSELL, M.J. (2003). Modeling tissue-specific signaling and organ function in three dimensions. J. Cell Sci. **116,** 2377–2388.

SHUCK, L., and ADVANI, S. (1972). Rheological response of human brain tissue in shear. J. Basic Eng. **94,** 905–911.

SIEG, F., WAHLE, P., and PAPE, H.C. (1999). Cellular reactivity to mechanical axonal injury in an organotypic *in vitro* model of neurotrauma. J. Neurotrauma **16,** 1197–1213.

SINGLETON, R.H., and POVLISHOCK, J.T. (2004). Identification and characterization of heterogeneous neuronal injury and death in regions of diffuse brain injury: evidence for multiple independent injury phenotypes. J. Neurosci. **24,** 3543–3553.

SMITH, D.H., WOLF, J.A., LUSARDI, T.A., LEE, V.M., and MEANEY, D.F. (1999). High tolerance and delayed elastic

response of cultured axons to dynamic stretch injury. J. Neurosci. **19,** 4263–4269.

THIBAULT, L.E., and GENNARELLI, T.A. (1989). Biomechanics of diffuse brain injuries. Presented at 10th International Tech. Conference on Experimental Safety Vehicles, DOT, NHTSA.

WINSTON, F.K., MACARAK, E.J., GORFIEN, S.F., and THIBAULT, L.E. (1989). A system to reproduce and quantify the biomechanical environment of the cell. J. Appl. Physiol. **67,** 397–405.

WOLF, J.A., STYS, P.K., LUSARDI, T., MEANEY, D., and SMITH, D.H. (2001). Traumatic axonal injury induces calcium influx modulated by tetrodotoxin-sensitive sodium channels. J. Neurosci. **21,** 1923–1930.

YAMADA, K.M., PANKOV, R., and CUKIERMAN, E. (2003). Dimensions and dynamics in integrin function. Braz. J. Med. Biol. Res. **36,** 959–966.

Address reprint requests to:
Michelle C. LaPlaca, Ph.D.
Georgia Institute of Technology
Coulter Department of Biomedical Engineering
313 Ferst Dr.
Atlanta, GA 30332-0535

E-mail: michelle.laplaca@bme.gatech.edu